Energy Saving Potential with a Double-Skin Roof Ventilated by Natural Convection in Djibouti

Abdou Idris Omar, Joseph Virgone, Etienne Vergnault, Damien David,
Abdoulkader Ibrahim Idriss

AiCARR 50th International Congress; Beyond NZEB Buildings, 10-11 May 2017, Matera, Italy

Energy Saving Potential with a Double-Skin Roof Ventilated by Natural Convection in Djibouti

Abdou Idris Omar[a,b,]*, Joseph Virgone[a], Etienne Vergnault[a], Damien David[a], Abdoulkader Ibrahim Idriss[b],

[a]*Université de Lyon, CNRS, Université Lyon 1, INSA-Lyon, CETHIL UMR 5008, Villeurbanne, France*
[b]*Université de Djibouti, Faculté d'Ingénieurs, GRE, Djibouti, Djibouti*

Abstract

In the Sub-Saharan African countries like Djibouti, the energy situation, the high rate of urban areas growth and the inadequate techniques of construction offer an exciting potential for the bioclimatic approach and sustainable construction. However, this poorly explored potential requires an investigation of different construction types in Djibouti and a good knowledge of the behavior of buildings components. Further a low energy building can be obtained because of the good realization of all its components. In fact, roofs call for attention as they represent a large part of a building's total surface area and amount of absorbed solar radiation. The goal of this paper is to investigate the benefit of using double skin-ventilated roofs for reducing cooling load under the Djiboutian climate. It is a first step towards ideas that will transform local construction practices to make them effective in energy, economic and functional dimensions. During investigation, we compared a ventilated roof assembly with traditional configuration after that the consistency of our model was validated with experiment of the literature findings. The computational fluid dynamics (CFD) model has been used for the characterization of the airflow and heat transfer phenomena in the ventilation cavity and provide fundamental information about the thermal performance of the roof. The results show the amount of the energy saving obtainable by the double-skin ventilated roof.
© 2017 The Authors. Published by Elsevier Ltd.
Peer-review under responsibility of the scientific committee of the AiCARR 50th International Congress; Beyond NZEB Buildings.

Keywords: Natural convection; double-skin roof; Energy saving; CFD

* Corresponding author. Tel.: +25377823879.
E-mail address: abdou.idris-omar@insa-lyon

1. INTRODUCTION

Demands of economic growth and improvements in living standards people led to higher levels of energy consumption. To speed up economic activities' development with less energy, efforts must focus on energy buildings efficiency, particularly, in country like Djibouti with important level of solar radiation. The axes of research stretch from envelope to diverse types of mechanical equipment and the bioclimatic conception of the building. The ventilated roof is one of the construction method used to reduce envelope gains of building by creating an air gap over the conventional roof. By the shading effect and the free ventilation in the air gap, this structure reduces the heat flux into the building. The study aims to examine the potential benefits of a ventilated roof under the Djiboutian climate

---

Nomenclature

Es   Energy saving rate
Cp   Specific heat at constant pressure J/(kg.K)
g   Gravity acceleration constant m/s²
d   roof width m
I   solar radiation W/m²
hc   convective heat transfer coefficient between outdoor air and screen W/(m². K)
heq   convective heat transfer coefficient including the effects of radiation and convection upon the screen W/(m². K)
hi   convective heat transfer coefficient between indoor air and ceiling W/(m².K)
T   temperature K
Ta   outdoor air temperature K
Ti   indoor air temperature K
Tsky   sky temperature K
v   air velocity field m/s
P   pressure Pa
t   Time [s]
y   y-axis perpendicular to the sreen
Greek symbols
β Gas expansion coefficient K-1
λ Thermal Conductivity W/m·K
ε surface emissivity
μ dynamic viscosity Pa.s
ρ density kg/m3
θ roof slope °
σ Stefan–Boltzmann constant: σ = 5.67E-8 W/(m2. K4)
Subscripts
us   Characteristic at the screen external surface
ls   Characteristic at the sheet metal surface
Superscripts
e   external surface
i   internal surface

2. Problem statement and approach

2.1. Problem statement

Measurements made by the Djiboutian Agency for Energy Management (ADME) [1], estimates the final energy consumption of the country at approximately 228 ktoe, distributed among the sectors as shown in Fig. 2-a. Transportation represents the largest share of consumption (81%) while the combined residential and tertiary sectors represent 18%. However, when only the electricity is considered, the building sectors represent the largest share, about 90% of the country's consumption as shown in Fig. 1-b.
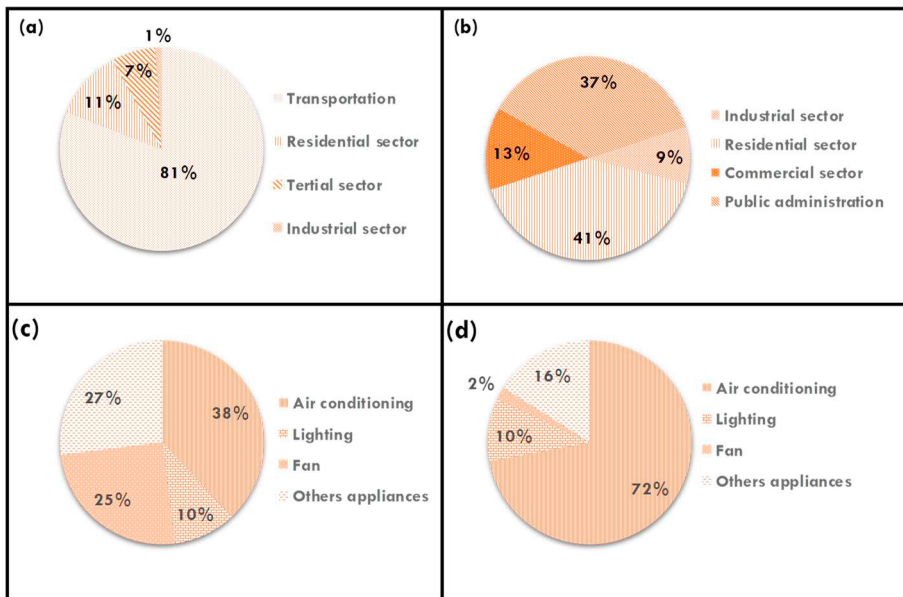

Fig. 1. Data surveys from Djiboutian Agency for Energy Management, (a) Sectoral distribution of electricity consumption in Djibouti; (b) Sectoral distribution of final energy consumption in Djibouti; (c) Breakdown of electricity consumption by use of households-2013; d) Breakdown of electricity consumption by use in administrative buildings-2013

The break-down of the electricity use in 2013 shows that in most buildings (office and household) high electricity consumption results from the use of air conditioning as shown in the Fig. 1 (c) and Fig. 1 (d). Electrical demand remains dominated by the refresh requirement, namely air conditioning and ventilation, which together account for more than 50% of electricity consumption. Indeed, cooling is one of the basic requirements for people because of the overheating of indoor spaces which is the major cause of human discomfort. But, in Djibouti, the need of air-conditioning is a serious financial problem for households and for the state and it is exacerbated by other factors like inefficiency of the building's envelope. In fact, if the building envelope is not correctly designed the heat fluxes through the structures are the cause of a significant increase in energy consumptions [2].
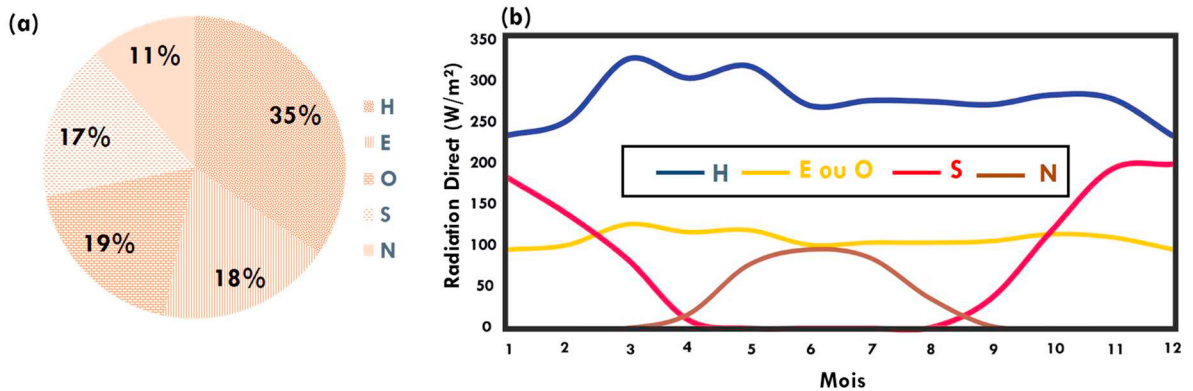
Fig. 2. Annual breakdown of direct radiation on horizontal roof and oriented walls; (b) Direct solar radiation on horizontal roof and different orientated walls

The amount of solar energy received by the surface depends on the sun position and the time of day or the time of year. The data collected from a local weather station were used to estimate the heat gain for each surface as shown in Fig. 2 (a). The Figure 2 - b show the amount of monthly average direct radiation on a horizontal roof and vertical wall, for different orientations in Djibouti. The roof receives the largest part of the solar radiation with nearly 35% of the total radiation reaching the building. The south facing wall receives 17%, the north wall 11% and the east and west oriented wall receive 38% together. The heat is transferred through the wall into the building whose temperature increases. Therefore, the thermal efficiency of the roof is an essential element in providing thermal comfort. This depends mostly on the roof forms and the materials used to minimize the amount of solar radiation absorbed by the roof. In the ventilated roof, the heat is removed by the air flow through the double-skin and thus constitutes a cost effective for the developing country like Djibouti.

In Djibouti, building typology is classically centered on the development of two sectors: residential and tertiary. The residential sector is generally composed of the following types of buildings:

- Standard home made up of, in the most of case, sheet-metal roof or tiles roof. This type represents the largest share according to DISED, the Djiboutian agency of demographic and statistical data [3], with 67% of the residential sector as shown in Fig. 3 (a). An example of the building front face is presented in Fig. 3 (b) with a pitch angle of more than 5° at least.
- Residential building with 5% of the construction consists of several floor levels and a concrete roof.
- Villa with 4% is single family home with tiles roof or concrete roof.
- The walls of theses building consist of external and internal cement plaster and bricks or concrete blocks.
- Tukuls, informal settlements and others which together account for more than 20% constitute an extremely precarious building and are in the urban slum.
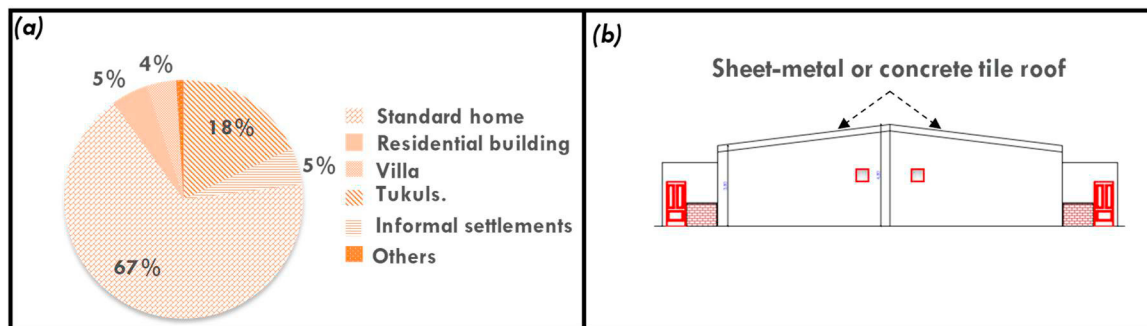
Fig.3. (a) Annual breakdown of direct radiation on horizontal roof and oriented walls; (b) Example of the building with the largest share

There is no trace of traditional architecture in Djibouti, which could have provided the basis for a sober bioclimatic architecture in term of resources use and energy consumption. Furthermore, the architecture of Djibouti is marked by the colonial past of the city and bears the early influences of the Yemenite architecture and the Arab cities with a large permanent and perpetual construction projects.

2.2. Literature review

Many researches have been undertaken to study the performance of a ventilated roof since Fracastoro et al. in 1997 [4] who studied the idea of reducing heat gain in dwellings by using under-roof cavities. They presented a numerical model for steady-state thermal analysis of ventilated and unventilated light roofs. Sandberg and Moshfegh in 1998 [5] has discussed about the relationship between the solar heat input and the induced cavity ventilation rate. In 2001, Hirunlabh et al. [6] tested different correlations for the Nusselt number as a function of solar radiation for different tilt angles of the roof. In 2002, the French Scientific and Technical Centre for Building Research [7] conducted a series of measurements on an experimental double-skin roof. Experimental investigation of free convection in roof solar collector by Khedari et al in 2002 [8] resulted in a dependence law of the Nusselt number upon the Rayleigh number, the angle of channel, and the aspect ratio of the ventilation cavity, i.e., the ratio between channel's width and its length. Ciampi et al. in 2005 [9], then, Dimoudi et al. 2006 [10] and Černe and Medved in 2007 [11], recognized that the ventilated roof contributes to maintain the temperature of the inner shell to a temperature that is closer to ambient conditions, and thereby reduce the impact of solar radiation on building. In 2007, Chang et al. [12] evaluated experimentally the energy savings achieved by incorporating a radiant barrier system in a double-skin roof. Based on numerical and experimental simulation, Biwole et al. in 2008 [13] stated that the optimal width for the ventilation channel must lie between 6 cm and 10 cm. Lai et al. in 2008 [14] investigated further the optimal spacing as a function of the Grashof number by using an open-ended inclined model with parallel plates to simulate the ventilated roof structure receiving solar radiation. Villi et al. [15] for their part, develop correlations for the characterization of the airflow and heat transfer phenomena in the ventilation cavity in 2009. Based on the study of the thermo-fluid dynamic behavior of the air within the ventilated roof and the heat fluxes through ventilated roofs, Gagliano et al. in 2012 [16] concluded that the ventilation of roofs can reduce significantly the heat fluxes (up to 50%) during summer season.

The study of the ventilated structures is very complex and depends on the airflow rate, thermo-physical properties of materials, external conditions and many other parameters. The aim of this is to investigate the thermal performance of ventilated roofs in Djibouti. The computational fluid dynamics (CFD) has been used for the characterization of the airflow and heat transfer phenomena in the ventilated cavity with buoyancy driven airflow. Experiment from the literature review has been used to validate the CFD model and then the energy performance has been evaluated for three configurations based on the dimensionless index (Es).

3. Numerical simulation description

3.1. Model description

The roof of standard house is studied here since it represents the largest part of the building typology in Djibouti. This type of home is generally built with peaked galvanized sheet roof or a tiled roof or just a concrete slab. Two model configurations to reduce the heat fluxes through the roof were considered. The first configuration is a ventilated structure consisting of two flat elements separated by an airgap that enable air flow as shown in Fig. 4. A 6-mm screen is placed over the standard roof (sheet metal). In the second configuration, a 5-cm insulation is added in the inner slab. The traditional inclination (5°) and 5-m length of the roof is assumed. All materials have also been assumed to be homogeneous and isotropic.
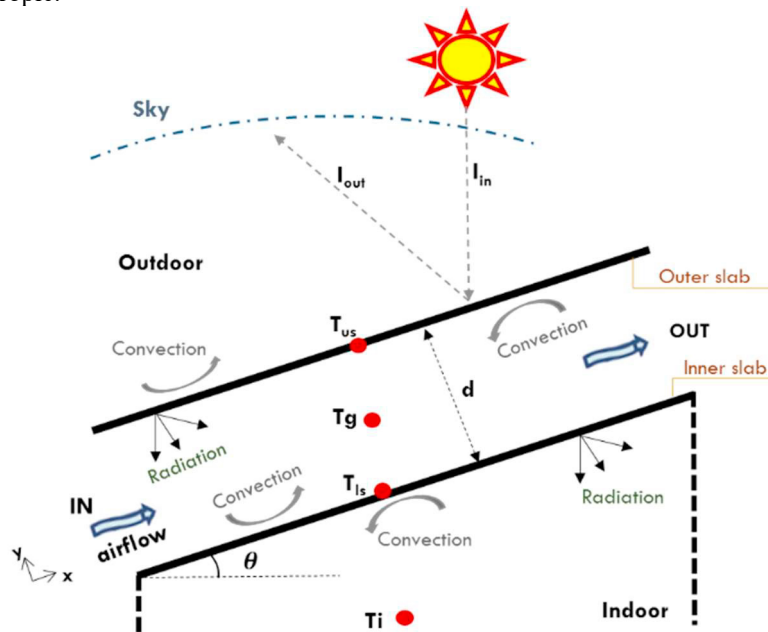

Fig.4. Schematic representation of the ventilated roof

Thermo-physical characteristics and geometry of the ventilated roofs are shown in   Table 1.

Table 1. Materials physical characteristics.

	Cp [J/kg.K]	λ [W/m.K]	ρ [kg/m3]	Thickness [m]
Sheet metal and screen	500	61	7520	0.006
Air cavity	1006	0.025	1.23	0.2
Insulation	1400	0.035	25	0.05

The roof is separated from the indoor by a non-ventilated air gap. The thermal resistance of the air gap has been evaluated to 0.18 m2/K.W, making reference to the ISO EN UNI 6946 guidelines [17] (CEN,2007).This value was also verified by CFD prediction.

3.2. Governing equations and Boundary conditions

In this study, the wind effect was ignored. Indeed, wind conditions in the urban environment are influenced by the local wind data, the density of the buildings in the area and wind canyon effects [17] which is a challenging task to reproduce. Therefore, only the flow of air due to difference in density resulting from being at different temperatures has been considered and the wind contribution has been assumed to be null, which corresponds to the worst case.

The computation fluid dynamic (CFD) approach has been used to calculate the thermodynamic properties of air within the ventilated layer via the "Fluent" code. It's a detailed modelling technique that solves the time averaged Navier–Stokes equations of motion for steady and incompressible flows. These equations are coupled to heat equation for analysis of thermal performances of ventilated roof.

Within the solid parts, (screen, sheet metal and insulation) heat transfers are dominated by conduction governed by the following equation (1):

$$\rho C_p \frac{\partial T}{\partial t} = \lambda \Delta T \tag{1}$$

where λ is the thermal conductivity, ρ is the density, C_p is the specific heat capacity, T and t refer to the temperature and the time.

Above the upper slab, this equation can be solved using the Neumann boundary condition as shown in equation (2).

$$\lambda_{us} \frac{\partial T}{\partial y} = h_c(T_a - T_{us}^e) + \varepsilon_{us}^e\left(T_{sky}^4 - T_{us}^{e\ 4}\right) + \alpha_{us}I \tag{2}$$

where T_{us}^e is the temperature of the upper slab's external surface and T_a is the outdoor air temperature, α_{us} is the solar absorption coefficient of the screen, I is the total solar radiation incident on the surface while h_c is the coefficient of convective heat transfer upon the screen. However, the problem has been simplified and the sol-air temperature (T_{sa}) has been calculated on the screen. The sol-air temperature allows considering the effect of the solar radiation incident on the external surface of the roof (Panatnia et al., 2010) (Ciampi et al., 2005) by the following equation (3):

$$T_{sa} = T_a + \frac{\alpha_{us}I}{h_{eq}} \tag{3}$$

where h_{eq} is the coefficient of heat transfer including the effects of radiation and convection upon the screen.

On the internal surface, convection with the air and long wave radiation with the lower slab are considered. Beneath the lower slab, long wave radiation with a non-ventilated cavity has been neglected. Such approximation is done because of the feeble impact of the long wave radiation on the air gap's temperature [13]. And the temperature of the cavity has been assumed to be equal to that of the room. Therefore, the following equation (4) is considered:

$$\lambda_{ls} \frac{\partial T}{\partial y} = h_i\left(T_i - T_{ls}^i\right) \tag{4}$$

where T_{ls}^i is the lower slab's indoor surface temperature.

The value of the solar absorption of the screen covering surface has been set to 0.6. Heat transfer coefficient of inner and outer surface have been defined respectively h_i= 7.8 W/(m².k), and h_{eq}= 12 W/(m².k), taking 313.15 K as outdoor temperature and 299.15 as indoor temperature. The emissivity of the two slabs facing the air gap has been assumed to 0.8.

In the air gap, heat equation (1) is coupled with:

✓ Conservation of mass
Since the density variation of the air in the cavity is supposed constant, this equation is simplified to

$$\nabla \vec{v} = 0 \qquad (5)$$

where $\vec{v}$ is the velocity vector in equation (5) and (6).

✓ Conservation of momentum (in the stationary case)

$$\rho \vec{v}.\nabla \vec{v} = \nabla (\mu(\nabla \vec{v} + (\nabla \vec{v})^{T}) - \nabla P + \rho \vec{g} \qquad (6)$$

where ρ is the air density, P is the static pressure, while $\rho \vec{g}$ represents the buoyancy force. The study of natural convection is made by the Boussinesq approximation using equation (7).

$$\rho = \rho_a \left(1 - \beta (T - T_a)\right) \qquad (7)$$

Therefor the buoyancy force from equation (6) becomes:

$$\rho \vec{g} = \rho_a \left(1 - \beta (T - T_a)\right)\vec{g} \qquad (8)$$

where ρ_a is the density at T_a and $\beta = \frac{1}{T_a}$ is the thermal expansion coefficient. To take in account the air inlet and outlet into the air gap, a constant temperature T_a and relative pressure of 0 Pa has been assigned at the entry and outlet.
    These equations are solved in a geometrical domain defined by the boundary conditions previously mentioned and taking into account turbulent phenomena. Turbulence modelling is particularly relevant in CFD simulation since unsuitable modeling may be an important source of error.
    The k-ε "realizable" model has been used in this study. The choice of this model is directly linked to his accuracy in flow inside cavity. Many reaserch find that this model has been validated for flows problems with pressure gradients and recirculation [19,20]. For a better understanding of wall-bounded flow, and in order to enable the full resolution of the viscosity dominated region, the near-wall region has been finely modeled. An example of the meshing for such process is displayed in Fig. 5.
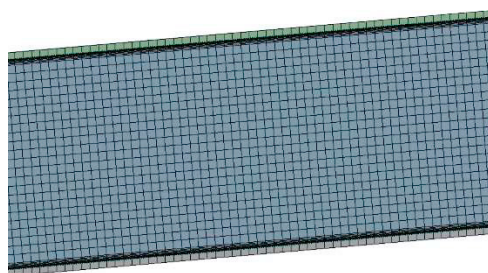

Fig. 5. Results of the meshing

The modeling of the near-wall flow consists in defining a numerical model using the enhanced wall treatment approach capable of predicting the pressure-velocity and temperature fields near the components of the roof which subdivide the domain into a viscosity affected region and a fully turbulent region. Therefore, to include the buoyancy effects on turbulent equations, the full buoyancy effect has been turned on.

The simulations were carried out by considering the air as a Newtonian fluid, incompressible, of constant viscosity and subjected to the gravity field. The discretization is based on the finite volume method and the resolution of the

equations is based on the SIMPLE algorithm. This algorithm based on a predictor-corrector method was developed by Patankar [21].

Convergence control has been carried out using convergence thresholds. These are residues resulting from the iterative resolution of the system of equations. For all the simulations, the values of these thresholds are the following:
- 10-4 for continuity,
- 10-3 for the turbulent kinetic energy and its dissipation rate,
- 10-6 for energy.

4. Validation of the cfd model

To evaluate the fluid dynamic model, the numerical simulations have been validated in comparison with experimental data from Biwole et al. 2008. The channel object of the experiment of Biwole et al. consisted of a 1-m large and long, 1.2 mm-wide sheet iron laid over a 3-cm-wide insulation with an air gap of 15 mm between sheet and insulation. Then an additional metal sheet was placed over the first one. To evaluate the accuracy of our computational model, to predict thermo-fluid dynamic phenomena in the ventilated cavity, numerous numerical simulations have been executed reproducing the same hypothesis of Biwole's experiments. The following Fig. 6 shows the results of the measurement performed on an hourly basis using the weather conditions registered on the 2nd of August 2006 inside the Scientific and Technical Centre for Building Research, Grenoble, France.
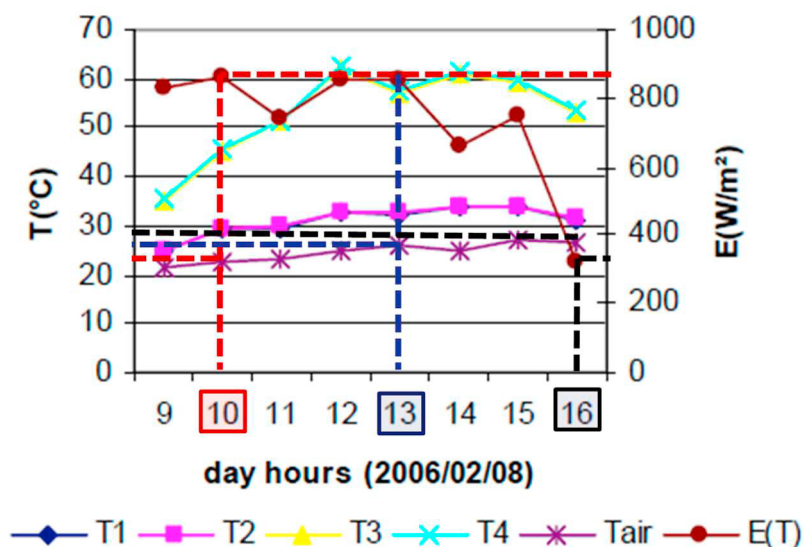

Fig. 6. Double-skin roof measured data (Biwole et al.,2008)

- T1 to T4 correspond to temperature measured by a T-type thermocouple with T4 placed on the external face of the upper sheet whereas T2 is placed on the cavity-side face of the lower sheet. E indicates the solar radiation and Tair, the outdoor air temperature. From this result, three points (at 10 a.m., 1 p.m. and 16 p.m.) has been used to validate the numerical simulation by comparing, each time, T2 and T4 to numerical result. The following Table II presents the comparison between experimental and numerical solution. It is interesting to note here that a noticeable difference between numerical and experimental results is observed at the early and late hours. The heat variations of the metal sheet are less rapid due to their thermal inertia which is not considered by our stationary numerical simulation. However, in the middle part of day, the numerical prediction shows the same variation of the

experimental results with a difference of 1°C or less in temperature. Based on these comparisons it is possible to assert the validity of the proposed CFD model for the study of ventilated structures.

Table 2. – Comparison between experimental and numerical results at various times.

	At 10 am (Ta =27°C ; E=885 W/m²)		At 13 pm (Ta =24°C ; E=885 W/m²)		At 16 pm (Ta =28.5°C ; E=370 W/m²)	
	Screen temperature (K)	Sheet iron	Screen temperature (K)	Sheet iron	Screen temperature (K)	Sheet iron
Experimental result	309	298	330.95	305.65	326	305
Numerical simulation result	329	304	332	306	318	303

5. Results and discussion

5.1. Temperature and air velocity fields

After the CFD model used in this study has been validated, the configurations of the roof described in the paragraph 2 is analysed from thermal performance point of view. In the section, only the configuration without insulation is presented. The second configuration with insulation is discussed in part 4.2. The following environmental conditions have been used for the simulation:
- Solar radiation I = 1000 W/m². This value corresponds the highest value in Djibouti according to our local weather station.
- Outdoor temperature Ta = 313 K;
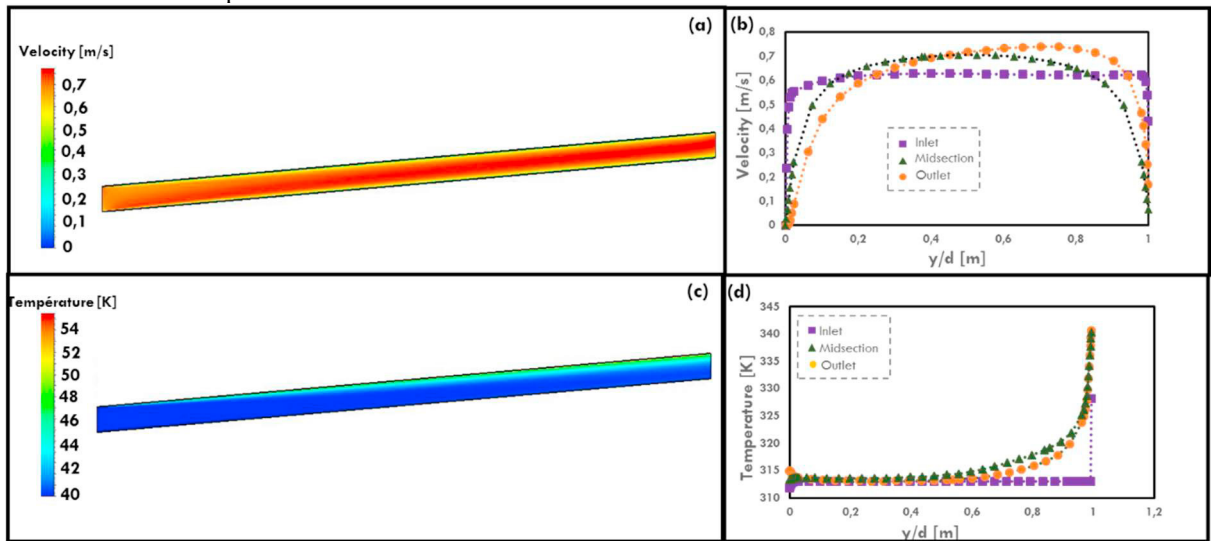- Indoor temperature Ti = 299 K.

Fig. 7. (a) Velocity contours; (b) Velocity's profiles on different cross-sections; (c) Temperature contours; (d) Temperature's profiles on different cross-sections

The temperature and air velocity profiles within the cavity are presented in Fig.7. These results concern only the ventilated roof in Fig. 4. The air velocity profile in Fig. 7 (b) is parabolic, with a zero value on both plates due to the no-slip boundary condition. However, the temperature in the cavity strongly increases reaching a maximum value of 340 K near the screen, thus forming an asymmetrical profile. The buoyancy force, which is proportional to the

difference between plate's temperature and outdoor temperature, causes this and the buoyancy is largest near the screen.

The air temperature increases along the direction of the motion as shown in the Fig. 7 (c) and 7 (d). It was also noted that the air in the middle of the airgap remains at the outdoor temperature for the simple reason that the thermal boundary layer of the two plates have not merged. The upper slab's temperature varies from 328 K to 340.5K whereas metal sheet's temperature varies from 311 to 315K due to thermal radiation and the lower values being observed near the channel's entry. This result is characteristic of natural convection flow within the ventilated cavity [13].

5.2. Heat flux through the roof structure

To have a quantitative assessment of the energy saving potential of the ventilated roof it is necessary to compare the heat flux incoming for three typologies of roof as shown in Fig.8. The first case (see Fig. 8 (a)) is the traditional galvanized sheet roof structure. The second case (see Fig. 8 (b)) corresponds to a non-insulated ventilated roof and the last case in Fig. 8 (c) is an insulated ventilated roof.
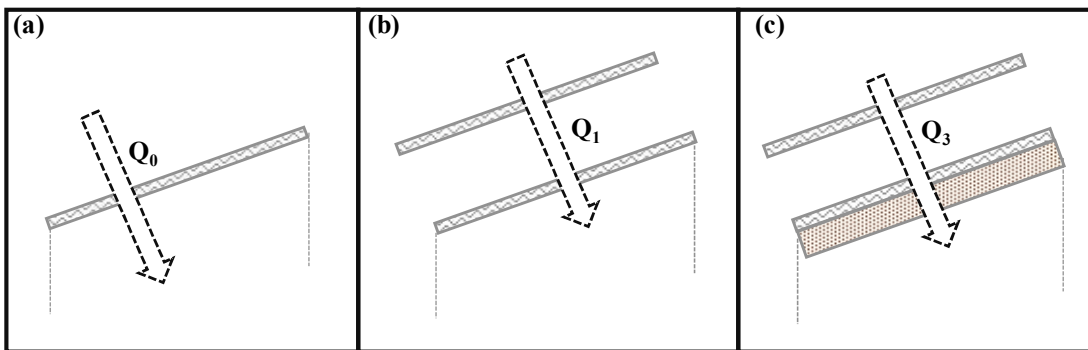

Fig. 8. Heat flux incoming for (a) standard roof; (b) ventilated roof; (c) ventilated and isolated roof

The thermal performance has been studied by introducing an indicator of performance, that enables the comparison between the two different ventilated roofs compared to the standard roof, which is the energy saving rate E_s defined as:

$$E_s = \frac{Q_{1\ or\ 2}}{Q_0} \tag{9}$$

where Q_0, Q_1 and Q_2 are the heat flux coming into the building, referred to a standard roof, to a ventilated but non-insulated roof and to ventilated and isolated roof. The results are presented in Fig. 9.
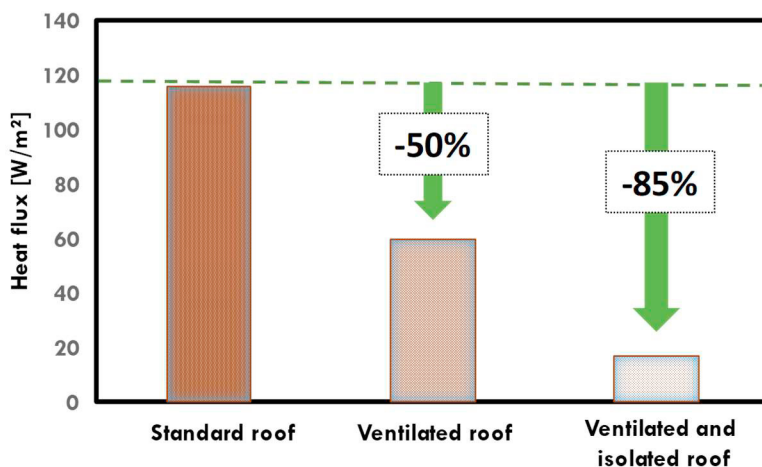
Fig. 9. Heat flux incoming for (a) standard roof; (b) ventilated roof; (c) ventilated and isolated roof

It is possible to observe that the use of the ventilated roof considerably reduces heat flux coming into the building (almost 50% of energy saving rate) from 116 W/m² for the standard roof to 60 W/m² for the ventilated but non-insulated roof. In case the roof has an insulation placed in the inner slab in addition of the ventilated cavity, the efficiency of the roof is even better than the previous configuration saving up to 85 % of the incoming heat flux with only 17 W/m². This result indicates that the ventilated and insulated roofs have the best performance, from the point of view of energy saving.

Acknowledgements

References

[1] ADME (Agence Djiboutienne de la Maitrise de l'Energie), 2013. Elaboration d'une stratégie et d'un plan d'action de maîtrise de l'énergie à Ministère de l'Energie encharge des Ressources Naturelles. Djibouti.

[2] Özdeniz M.B., Hanc P.. Suitable roof constructions for warm climates—Gazimagusa case, Energy and Buildings, 2005. 37:643–649.

[3] DISED (Direction de la statistique et des Etudes Démographiques). Annuaire Statistique. Djibouti. 2015.

[4] Fracastoro G. V., Glai L., Perino M.. Reducing cooling loads with under roof air cavities, in: Proceedings of AIVC 18th Conference, Ventilation and Cooling, Athens, Greece. 1997. p. 477-486.

[5] Sandberg M., Moshfegh B. Ventilated-solar roof airflow and heat transfer investigation, Renewable energy.1998. 15:287–292

[6] Hirunlabh J., Wachirapuwadon S., Pratinthong N., Khedari J. New configurations of a roof solar collector maximizing natural ventilation. Building and Environment. 2001. 36: 383 - 391.

[7] CSTB, Determination of the Thermal Performances of a Roof Ventilation System Grenoble, France., 2002. E-01-0005.

[8] Khedari J., Yimsamerjit P., Hirunlabh J. Experimental investigation of free convection in roof solar collector. Building and Environment.2002. 37: 455 − 459.

[9] Ciampi M., Leccese F., Tuono G. Energy analysis of ventilated and microventilated roofs. Solar Energy. 2005. 79: 183 − 192.

[10] Dimoudi A., Androutsopoulos A., Lykoudis S. Summer performance of a ventilated roof component. Energy and Buildings. 2006., 38: 610 − 617.

[11] Černe B., Medved S. Determination of transient two-dimensional heat transfer in ventilated lightweight low sloped roof using Fourier series. Building and Environment. 2007., 42: 2279 − 2288.

[12] Chang P-C, Chiang C-M, Lai C-M, Development and preliminary evaluation of double roof prototypes incorporating RBS (radiant

barrier system), Energy & Buildings. 2008.40:140–147.

[13] Biwole P.H., Woloszyn M., Pompeo C. Heat transfers in a double-skin roof ventilated by natural convection in summer time. Energy and Buildings. 2008.40: 1487 − 1497.

[14] Lai C., Huang J.Y., Chiou J.S. Optimal spacing for double-skin roofs. Building and Environment.2008, 40: 1749 -1754.

[15] Villi G., Pasut W., De Carli M. CFD modelling and thermal performance analysis of a wooden ventilated roof structure. Building Simulation 2. 2009., 215–228.

[16] Gagliano A., Patania F., Nocera F., Ferlito A. Galesi A., Thermal performance of ventilated roofs during summer period, Energy and Buildings. 2012. 49:611–618.

[17] CEN.2007. EN 6946—Building components and building elements - Thermal resistance and thermal transmittance—Calculation method. Brussels: European Committee for Standardization.

[18] Antvorskov S. Introduction to integration of renewable energy in demand controlled hybrid ventilation systems for residential buildings. Building and Environment. 2008. 43: 1350 − 1353.

[19] Shih T.H., Liou W.W., Shabbir A., Yang Z., Zhu J. A new k −ε eddy viscosity model for high Reynolds number turbulent flows. Journal Computers Fluids. 1995., Vol. 24, n°3, pp. 227-238.

[20] Teodosiu C. Modélisation des systèmes techniques dans le domaine des équipements des bâtiments à l'aide des codes de type CFD. Thèse MEGA. Lyon : INSA de Lyon. 2001. 355p

[21] Patankar S.V. Numerical Heat Transfer and Fluid Flow. Washington (United States): Mac Graw and Hill. 1980., 197p.